Metab Brain Dis (2016) 31:1303–1314
DOI 10.1007/s11011-015-9715-8

ORIGINAL ARTICLE

^{1}H and ^{31}P magnetic resonance spectroscopy in a rat model of chronic hepatic encephalopathy: in vivo longitudinal measurements of brain energy metabolism

Veronika Rackayova[1] · Olivier Braissant[2] · Valérie A. McLin[3] · Corina Berset[4] · Bernard Lanz[1] · Cristina Cudalbu[4]

Received: 18 May 2015 / Accepted: 26 July 2015 / Published online: 9 August 2015

Abstract Chronic liver disease (CLD) leads to a spectrum of neuropsychiatric disorders named hepatic encephalopathy (HE). Even though brain energy metabolism is believed to be altered in chronic HE, few studies have explored energy metabolism in CLD-induced HE, and their findings were inconsistent. The aim of this study was to characterize for the first time in vivo and longitudinally brain metabolic changes in a rat model of CLD-induced HE with a focus on energy metabolism, using the methodological advantages of high field proton and phosphorus Magnetic Resonance Spectroscopy (^{1}H- and ^{31}P-MRS). Wistar rats were bile duct ligated (BDL) and studied before BDL and at post-operative weeks 4 and 8. Glutamine increased linearly over time (+ 146 %) together with plasma ammonium (+159 %). As a compensatory effect, other brain osmolytes decreased: myo-inositol (-36 %), followed by total choline and creatine. A decrease in the neurotransmitters glutamate (-17 %) and aspartate (-28 %) was measured only at week 8, while no significant changes were observed for lactate and phosphocreatine. Among the other energy metabolites measured by ^{31}P-MRS, we observed a non-significant decrease in ATP together with a significant decrease in ADP (-28 %), but only at week 8 after ligation. Finally, brain glutamine showed the strongest correlations with changes in other brain metabolites, indicating its importance in type C HE. In conclusion, mild alterations in some metabolites involved in energy metabolism were observed but only at the end stage of the disease when edema and neurological changes are already present. Therefore, our data indicate that impaired energy metabolism is not one of the major causes of early HE symptoms in the established model of type C HE.

Keywords Type C hepatic encephalopathy · Bile duct ligation · Proton magnetic resonance spectroscopy · Phosphorus magnetic resonance spectroscopy · Energy metabolism · in vivo

Introduction

Type C hepatic encephalopathy (HE), also sometimes called chronic HE (CHE), is a serious neuropsychiatric disorder associated with chronic liver disease (CLD) (Ferenci et al. 2002). Neuropsychological manifestations vary from minimal to overt HE (Blei and Córdoba 2001). Despite persistent research in the last decades, the molecular pathogenesis of HE remains unclear, especially the molecular mechanisms underlying mild brain edema present in both animal models (Davies et al. 2009; Bosoi et al. 2011) and patients with CLD (Córdoba et al. 2001; Häussinger 2006; Kale et al. 2006; Shah et al. 2008).

It is commonly accepted in CLD that increased brain ammonia generates an osmotic stress caused by a rise in brain glutamine, only partially compensated by the gradual release of other brain osmolytes from astrocytes (primary myo-inositol but also total choline, taurine and creatine)

✉ Cristina Cudalbu
cristina.cudalbu@epfl.ch

[1] Laboratory of Functional and Metabolic Imaging (LIFMET), Ecole Polytechnique Fédérale de Lausanne (EPFL), Lausanne, Switzerland

[2] Service of Biomedicine, University Hospital of Lausanne, Lausanne, Switzerland

[3] Swiss Center for Liver Disease in Children, Department of Pediatrics, University Hospitals Geneva, Geneva, Switzerland

[4] Centre d'Imagerie Biomedicale (CIBM), Ecole Polytechnique Fédérale de Lausanne (EPFL), Lausanne, Switzerland

(Brusilow and Traystman 1986; Cooper and Plum 1987; Kreis et al. 1991; Häussinger et al. 2000; Butterworth 2003; Brusilow et al. 2010; Cudalbu 2013; Braissant et al. 2013) the result of which is mild brain edema. Several other pathways were proposed for edema formation, different from glutamine accumulation. Among these, cerebral energy metabolism is believed to be altered in both acute and chronic HE (Rama Rao and Norenberg 2012; Schousboe et al. 2014; Ott and Vilstrup 2014). But the direct role of energy impairment in the development and progression of brain edema is not firmly established. Ammonium is a neurotoxin causing numerous toxic effects on cerebral metabolism which may interfere with energy pathways. Moreover, it has been postulated that glutamine increase, generated by a rise in circulating ammonium, could secondarily impact energy metabolism in one of several ways: through an initial osmotic stress, through changes in the glutamate-glutamine cycle, or by the deleterious effects of cytotoxic brain edema at later stages of the disease (Zwingmann and Butterworth 2005). Compared to acute liver failure in which energy metabolism has been described in more details (i.e. compromised TCA cycle due to inhibition of α-ketoglutarate dehydrogenase, limited anaplerotic flux and capacity of astrocytes to detoxify ammonium by glutamine synthesis, increased lactate synthesis and mitochondrial permeability transition induced by oxidative/nitrosative stress (Lai and Cooper 1991; Ott et al. 2005; Zwingmann and Butterworth 2005; Zwingmann 2007; Rama Rao and Norenberg 2012)), findings on energy metabolism disturbances in CHE are not consistent. There are only a few studies examining energy metabolism in either patients or animal models of HE due to CLD, showing decreased cerebral metabolic rate for glucose in CHE patients (Hazell and Butterworth 1999) and decreased cerebral oxygen consumption and blood flow in cirrhotic patients (Dam et al. 2013).

Further, to the best of our knowledge, no in vivo longitudinal studies have been performed in experimental animal models of CLD measuring the kinetics of brain energy metabolism. In this context, magnetic resonance spectroscopy (MRS) is a unique technique allowing the non-invasive study of brain metabolism both in vivo and longitudinally. High magnetic fields enable the detection of additional brain metabolites and thus the pathogenic mechanisms involved in HE can be more accurately assessed. High field proton (^{1}H) MRS, characterized by its excellent spectral resolution, provides information about amino acid disturbances, alterations in neurotransmitters, oxidative stress, osmoregulation, myelination/cell proliferation and disturbances in cerebral energy metabolism (McPhail et al. 2012; Cudalbu 2013). Phosphorus (^{31}P) MRS is very useful for the study of in vivo energy metabolism by providing information on the energy status of phosphate compounds and phospholipid metabolism. There are some previous studies investigating cerebral energy metabolism in CLD patients at low magnetic field using ^{31}P-MRS, but their findings are discordant (Taylor-Robinson et al. 1996, 1999; Bluml et al. 1998; Barbiroli et al. 2002).

The purpose of this study was to investigate brain metabolism in vivo and longitudinally in a rat model of CLD-induced HE with a specific focus on energy metabolism. For this we used in vivo ^{31}P-MRS at 9.4Tesla to study high energy metabolites. This approach was combined with ^{1}H-MRS to measure brain glutamine and other metabolites involved in osmoregulation, neurotransmission or energy metabolism. The novelty of this study relies on the in vivo, non-invasive and longitudinal measurements at a very high magnetic field offering unprecedented molecular resolution into brain energy metabolism in CLD-associated HE.

Methods

Animal model

Wistar male adult rats (n=7, 150–175 g, Charles River Laboratories, L'Arbresle, France) underwent bile duct ligation (BDL) as previously described (Biecker et al. 2005). According to ISHEN (International Society for Hepatic Encephalopathy and Nitrogen Metabolism) commission, the BDL rat model reflects HE associated with cirrhosis, portal hypertension and hyperammonemia (Butterworth et al. 2009). MRS measurements were performed in vivo and longitudinally before BDL (week 0) and at post-operative weeks 4 and 8 (week 4 and week 8). Therefore, each animal served as its own control. For all the MRS procedures, animals were anesthetized using 1.5–2 % of isoflurane in 100 % oxygen. Anesthesia is often a requirement for MR studies to minimize movement and also to prevent unnecessary stress to animals. Since all MRS measurements were performed under anesthesia also before BDL (week 0), all our results were presented as relative changes compared to the pre-operative scan. Respiration rate was maintained at 60–70 breaths/min and body temperature at 37.5–38.5 °C. Animals had unrestricted access to standard rat chow and water ad libitum for the duration of study. All procedures were approved by the Committee on Animal Experimentation for the canton of Vaud, Switzerland.

Biochemical measurements

Blood samples were taken from the sublingual vein before BDL and at post-operative weeks 4 and 8. Plasma ammonium, total and direct bilirubin, alanine aminotransferase (ALAT) and γ-glutamyl transferase (γ-GT) as markers of liver function were measured for all rats at all time-points on an Integra©, respectively a COBAS8000©, automates (Roche, Switzerland).

In vivo Magnetic Resonance Spectroscopy (MRS)

In vivo ^{1}H- and ^{31}P-MRS measurements were performed on a horizontal actively shielded 9.4Tesla system (Magnex Scientific, Oxford, UK) interfaced to a Varian Direct Drive console (Palo Alto, CA, USA). A home-built dual transceive surface coil was used, consisting of a ^{1}H-quadrature coil (17 mm diameter for each loop) placed above a linearly polarized 15 mm diameter ^{31}P-coil. Anatomical T_2 weighted images (multislice turbo-spin-echo sequence, with repetition time/effective echo time (TR/TE_{eff})=4000/52 ms, echo train length=8, field of view=23 mm×23 mm, slice thickness= 1 mm, 2 averages, 128^2 image matrix) were acquired in the axial plane to position the volume of interest (VOI) of 4×7.5× 6.5 mm^3 in the middle part of the brain containing different brain regions (cortex, hippocampus, striatum). This bigger region non-specific VOI was needed to increase the lower intrinsic sensitivity of ^{31}P-MRS compared to ^{1}H-MRS. First and second order shims were adjusted using FAST(EST)MAP (Gruetter and Tkác 2000) until reaching water resonance linewidth of 15-18Hz. ^{1}H localized spectra were acquired using the ultra-short-echo time SPECIAL spectroscopy sequence (TE=2.8 ms, TR=4 s, 80 averages) (Mlynárik et al. 2006). To improve signal localisation, outer volume suppression (OVS) was used and interleaved with water signal suppression by variable power RF pulses with optimized relaxation delays (VAPOR) (Tkáč et al. 1999).

Metabolite concentrations were calculated by LCModel (Provencher 2001) using an in vitro measured basis set of metabolites and the spectrum of macromolecules measured in vivo (Cudalbu et al. 2012). The ultra-short TE allowed the in vivo detection of 20 metabolites, which were all included in the basis set: alanine (Ala), ascorbate (Asc), aspartate (Asp), β-hydroxybutyrate (bHB), glycerophosphocholine (GPC), phosphocholine (PCho), creatine (Cr), phosphocreatine (PCr), γ-aminobutyric acid (GABA), glucose (Glc), glutamine (Gln), glutamate (Glu), glutathione (GSH), myo-inositol (Ins), lactate (Lac), N-acetylaspartate (NAA), N-acetylaspartylglutamate (NAAG), phosphoethanolamine (PE), scyllo-inositol (Scyllo) and taurine (Tau). Absolute metabolite concentrations were obtained using the unsuppressed water signal from the same VOI as an internal reference. The Cramer-Rao lower bounds (CRLB) were used as a reliability measure for the metabolite concentration estimate. Only metabolites with CRLB lower than 30 % were considered in each measurement.

For ^{31}P-MRS, a non-selective adiabatic half passage pulse was used for excitation and localization was performed with OVS in x-, y- and z-direction, together with a one dimensional ISIS in y-direction (TR=5 s, 640 averages) (Mlynárik et al. 2012). VOI and shimming procedure were the same as for ^{1}H scans. ^{31}P-MR spectra were quantified using AMARES (Vanhamme et al. 1997) from the jMRUI software (http://www.mrui.uab.es/mrui/). Absolute PCr concentration measured in the same VOI by ^{1}H-MRS and estimated by LCModel was used as a concentration reference to calculate metabolite absolute concentrations in ^{31}P-MR spectra. All metabolites were corrected for longitudinal (T_1) relaxation based on published T_1 relaxation constants (Tkac et al. 2012).

The high field ^{31}P-MRS allowed to assess cell membrane anabolic precursors and catabolic metabolites: phosphomonoesters (PME) represented mainly by PE and PCho and phosphodiesters (PDE) represented by GPC, all of which potentially containing small contributions of other PME or PDE; high energy phosphates (nucleoside triphosphates (NTP) and PCr) as well as inorganic phosphate (Pi) and nicotinamide adenine dinucleotide and nicotinamide adenine dinucleotide phosphate (NAD+NADP) resonance (both oxidized and reduced form) (Tkac et al. 2012; Mlynárik et al. 2012). The NTP resonances contain mostly ATP signal and thus are further presented as γ-, α-, and β-ATP resonances. Using these signals, other calculated parameters of energy metabolism as ADP concentration, pH, [Mg^{2+}], phosphorylation potential (PP), percentage of the maximal rate of ATP biosynthesis ($v/V_{max\text{-}ATP}$) and the relative rate of CK reaction ($v/V_{max\text{-}CK}$) were estimated as described in the appendix.

Statistical analysis

All results are presented as mean±SD. One way ANOVA (Prism 5.03, Graphpad, La Jolla CA USA) with time as repeated factor and followed by the Bonferroni's multi-comparisons post-test was used to assess significance ($p<0.05$) in metabolite's changes and calculated energetic parameters. Pearson correlation analysis was performed on all longitudinally acquired data to test for correlations between brain metabolites, plasma values and calculated energetic parameters.

Results

Biochemical measurements

At the time of sacrifice, all BDL rats presented clinical signs of cirrhosis: jaundice, ascites, hepatomegaly (liver weight=24.4 ±4.2 g in BDL rats as compared to 11±1.9 g in sham operated animals at corresponding age) and macroscopic cirrhosis. To confirm the presence of CLD in BDL animals, total and direct bilirubin, ammonium, ALAT and γ-GT were measured in plasma before BDL and at post-operative weeks 4 and 8. All BDL rats had plasma parameters in the normal range before BDL and showed a gradual increase in ammonium (from 60.6 ±11.7 to 157±100 μM, $p=0.02$), total and direct bilirubin (from non-measurable to 107±17 μM and 105±14 μM respectively, $p<0.0001$ for both), γ-GT (from non-measurable

to 55.0±27.4 IU/l, $p<0.0001$) and ALAT (from 44.0±6.7 to 61.1±32.7 IU/l, $p=0.06$) (Fig. 1).

Magnetic Resonance Spectroscopy (MRS)

^{1}H- and ^{31}P-MR spectra exhibited excellent signal-to-noise ratio (SNR) throughout the study. There was clear separation of Gln and Glu, as well as Cr and PCr, resonances in proton spectra at all time points. In total, 15 metabolites were precisely quantified in ^{1}H-MRS and 7 metabolites in ^{31}P-MRS. The bHB and Scyllo signals were included in the basis set but their concentrations were not reliably estimated (CRLBs >30 %). Moreover, an increase in water linewidth was observed 8 weeks after surgery probably due to disease evolution, which decreased the precision in quantifying metabolites at low concentrations (Ala, Glc, GPC and GSH (CRLBs >30 %)). Consequently, the concentration of these metabolites was not reported at week 8. Figure 2 shows typical brain ^{1}H- and ^{31}P-spectra from a BDL rat over the course of 8 weeks.

^{1}H-MRS brain metabolites

^{1}H-MRS showed important changes in brain osmolytes and neurotransmitters (Fig. 3). A gradual increase in Gln (+146 % weeks 8 vs 0, $p<0.0001$) was followed by the decrease in Ins (−36 % weeks 8 vs 0, $p=0.0001$). tCho (GPC+PCho) showed a smaller decrease at week 8 (-21 %, $p=0.043$). Cr, known for its role both in energy metabolism and osmoregulation (Bothwell et al. 2002) showed a tendency of decrease at week 8 (-11 %, $p=0.063$). Regarding the neurotransmitters, Glu (-17 %, $p=0.015$) and Asp (-28 %, $p=0.002$) showed a decrease at week 8.

Among metabolites involved in energy metabolism Lac showed a small increase at week 8 although this did not reach statistical significance (+18 %, $p=0.08$). Moreover, while Cr showed a −10 % decrease, PCr displayed no changes throughout the course of the study (Fig. 3). Glc and Ala tended to decrease at week 4 without reaching significance (-28 % and -27 % respectively), but their concentration was not reliably estimated at week 8.

GSH and Asc are important antioxidants protecting against oxidative stress. Asc showed no changes while GSH showed a -41 % decrease at week 4 without reaching statistical significance.

Finally, NAA, a metabolite believed to be a marker of neuronal function/density (Rae 2014) did not display any modifications during the study.

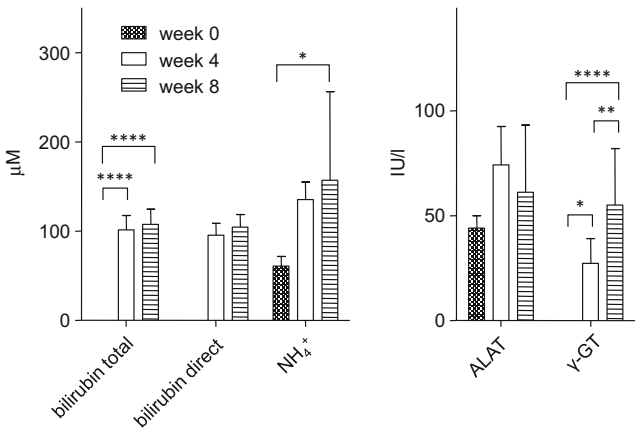

Fig. 1 Blood parameters. Levels of total and direct bilirubin, ammonium (NH_4^+), alanine aminotransferase (ALAT) and γ-glutamyl transferase (γ-GT) in plasma before BDL and at post-operative weeks 4 and 8 presented as mean±SD; values of total and direct bilirubin and γ-GT were non-measurable at week 0; significance level: *$p<0.05$, **$p<0.01$, ****$p<0.0001$

^{31}P-MRS metabolites

PE, PCho, GPC, Pi and NAD+NADP concentrations remained constant throughout the study. The ATP signal contains resonances from γ-, β- and α-ATP. To increase the reliability of ATP estimation, we only reported the concentration of γ-ATP in the present study, since α-ATP is slightly overlapping with NAD+NADP resonance and β-ATP was not fully excited by the RF pulse. ATP concentration tended to decrease only at week 8, on average by −10 % ($p=0.07$). The time evolution of PE, PCho, PCr in the ^{31}P-MRS spectra was very similar to the ones observed in ^{1}H-MRS spectra.

BDL rats showed a subtle decrease in cerebral pH starting at week 4, estimated to be the equivalent of a 0.03 pH decrease ($p=0.002$) at week 8. No significant change in [Mg^{2+}] was observed. Calculated ADP values showed a gradual decrease reaching −28 % at week 8 ($p=0.003$). It is important to emphasize that the apparent equilibrium constant of creatine kinase reaction (K_{CK}), necessary for ADP concentration calculation, is very sensitive to [Mg^{2+}] and pH. Thus its value was adjusted individually for each rat to actual ionic conditions based on the observed [Mg^{2+}] and pH values using published formulas (Golding et al. 1995). Our K_{CK} constants were 60.5±4.

No significant change was found in mean values for the high energy phosphate pool represented by PP, while high variability between BDL rats was observed at week 8. $v/V_{max\text{-}ATP}$ was constant over time in all animals, reaching values near to 100 % throughout the 8 weeks, while a significant decrease in $v/V_{max\text{-}CK}$ (-18 %, $p=0.012$) was measured in BDL rats at 8 weeks.

Correlations between brain metabolites and plasma values

Pearson correlation coefficients (r) were calculated to identify linear dependencies between estimated brain metabolite concentrations and plasma values using all time points. Figure 4 shows the most important correlations across all BDL rats at all time-points with the corresponding linear fits and the 95 %

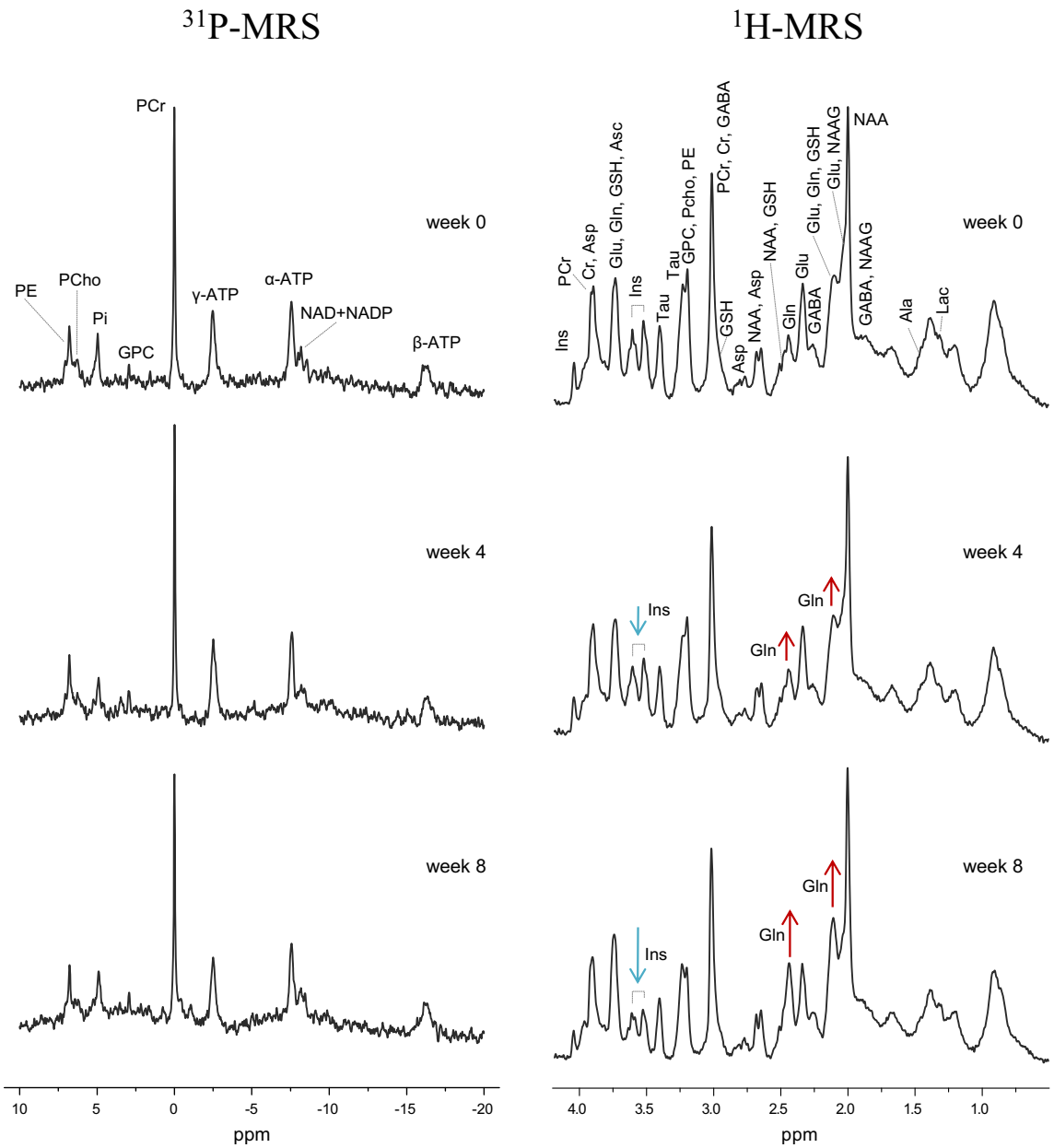

Fig. 2 Representative in vivo brain ^{1}H- (*left column*) and ^{31}P- (*right column*) MR spectra acquired at 9.4Tesla from the same rat measured before BDL (*first row*) and at post-operative weeks 4 (*second row*) and 8 (*third row*); the increase in Gln (highlighted with *red arrow*) and decrease in Ins (highlighted with *blue arrow*) throughout the evolution of the disease is clearly visible in the spectra; alanine (Ala), ascorbate (Asc), aspartate (Asp), glycerophosphocholine (GPC), phosphocholine (PCho), creatine (Cr), phosphocreatine (PCr), γ-aminobutyric acid (GABA), glucose (Glc), glutamine (Gln), glutamate (Glu), glutathione (GSH), myo-inositol (Ins), lactate (Lac), N-acetylaspartate (NAA), N-acetylaspartylglutamate (NAAG), phosphoethanolamine (PE), taurine (Tau), inorganic phosphate (Pi), adenosine triphosphate (ATP) and nicotinamide adenine dinucleotide (NAD), nicotinamide adenine dinucleotide phosphate (NADP)

confidence intervals. Since ammonium is considered to be responsible for many of the changes in HE, we evaluated the potential correlations between plasma ammonium and all other plasma and brain metabolites. We identified significant correlations with the following plasma values: total bilirubin (p=0.002) and γ-GT (p=0.03), and brain: Gln (p=0.007), Ins (p=0.02), Glu (p=0.03), ADP (p=0.01), pH (p=0.03) and $v/V_{max\text{-}CK}$ (p=0.03). As illustrated in Fig. 4, Gln, considered as ammonium chief's metabolite, displayed similar correlations with the above. Moreover, Gln displayed further correlations with tCho (p=0.009), Cr (p=0.005) and Asp (p=0.0004). In addition, ADP correlated with ATP (p=0.002), pH (p=0.002), $v/V_{max\text{-}CK}$ (p 0.0001), Glu (p<0.0001), Asp (p=0.003), Ins (p=0.0005) and Cr (p<0.0001).

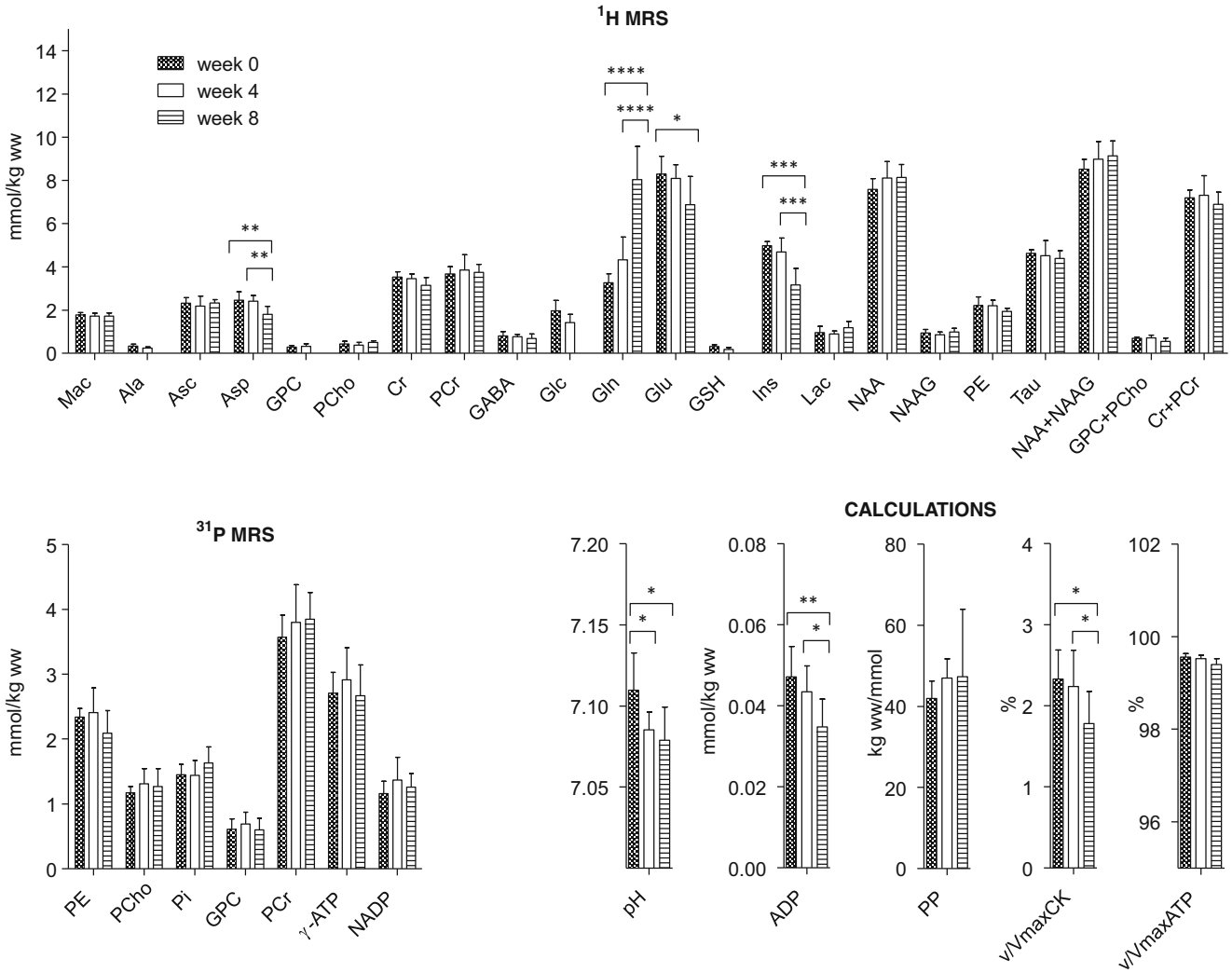

Fig 3 Brain metabolites and brain energy metabolism parameters. Time evolution of brain metabolites measured by ^{1}H-MRS (*top row*), measured by ^{31}P-MRS (*bottom row*) and evolution of calculated parameters of energy metabolism (*bottom row*); data presented as mean±SD; significance level: *$p<0.05$, **$p<0.01$, ***$p<0.001$, ****$p<0.0001$; alanine (Ala), ascorbate (Asc), aspartate (Asp), glycerophosphocholine (GPC), phosphocholine (PCho), creatine (Cr), phosphocreatine (PCr), γ-aminobutyric acid (GABA), glucose (Glc), glutamine (Gln), glutamate (Glu), glutathione (GSH), myo-inositol (Ins), lactate (Lac), N-acetylaspartate (NAA), N-acetylaspartylglutamate (NAAG), phosphoethanolamine (PE), taurine (Tau), inorganic phosphate (Pi), adenosine triphosphate (ATP) and nicotinamide adenine dinucleotide (NAD), nicotinamide adenine dinucleotide phosphate (NADP), adenosine diphosphate (ADP), phosphorylation potential (PP), relative rate of creatine kinase reaction ($v/V_{max\text{-}CK}$), relative rate of oxidative phosphorylation ($v/V_{max\text{-}ATP}$)

Discussion

The present study combines high field ^{31}P- with ^{1}H-MRS to study, for the first time, brain energy metabolism both *in vivo* and longitudinally in a rat model of type C HE. In addition, these methodological advantages offer the opportunity to study changes in osmolytes, neurotransmitters and other metabolites and correlate them with changes in energy metabolism. The few previous studies exploring energy metabolism in CLD were designed to measure single time-points rather than temporal modifications (Bluml et al. 1998; Taylor-Robinson et al. 1999). Therefore, little is known about early molecular and energy events in CLD, something which this study was designed to examine.

Our longitudinal ^{1}H-MRS measurements confirmed the characteristic increase in brain Gln associated with liver

Fig. 4 Correlations between blood parameters, brain metabolites and calculated parameters of brain energy metabolism. *First column*: Correlations between brain Gln and various CNS metabolites (brain osmolytes (Ins, GPC+Pcho, Cr), neurotransmitters (Asp, Glu), brain ADP and brain pH). *Second column*: Correlations between plasma ammonium levels and the same metabolites as for Gln (brain osmolytes (Ins, GPC+Pcho, Cr), neurotransmitters (Asp, Glu), brain ADP and brain pH). *Third column*: Correlations between various energy metabolites and parameters. Adenosine diphosphate (ADP), adenosine triphosphate (ATP), ammonium (NH_4^+), aspartate (Asp), creatine (Cr), glutamine (Gln), glutamate (Glu), glycerophosphocholine (GPC), phosphocholine (PCho), myo-inositol (Ins), relative rate of creatine kinase reaction ($v/V_{max\text{-}CK}$) ▶

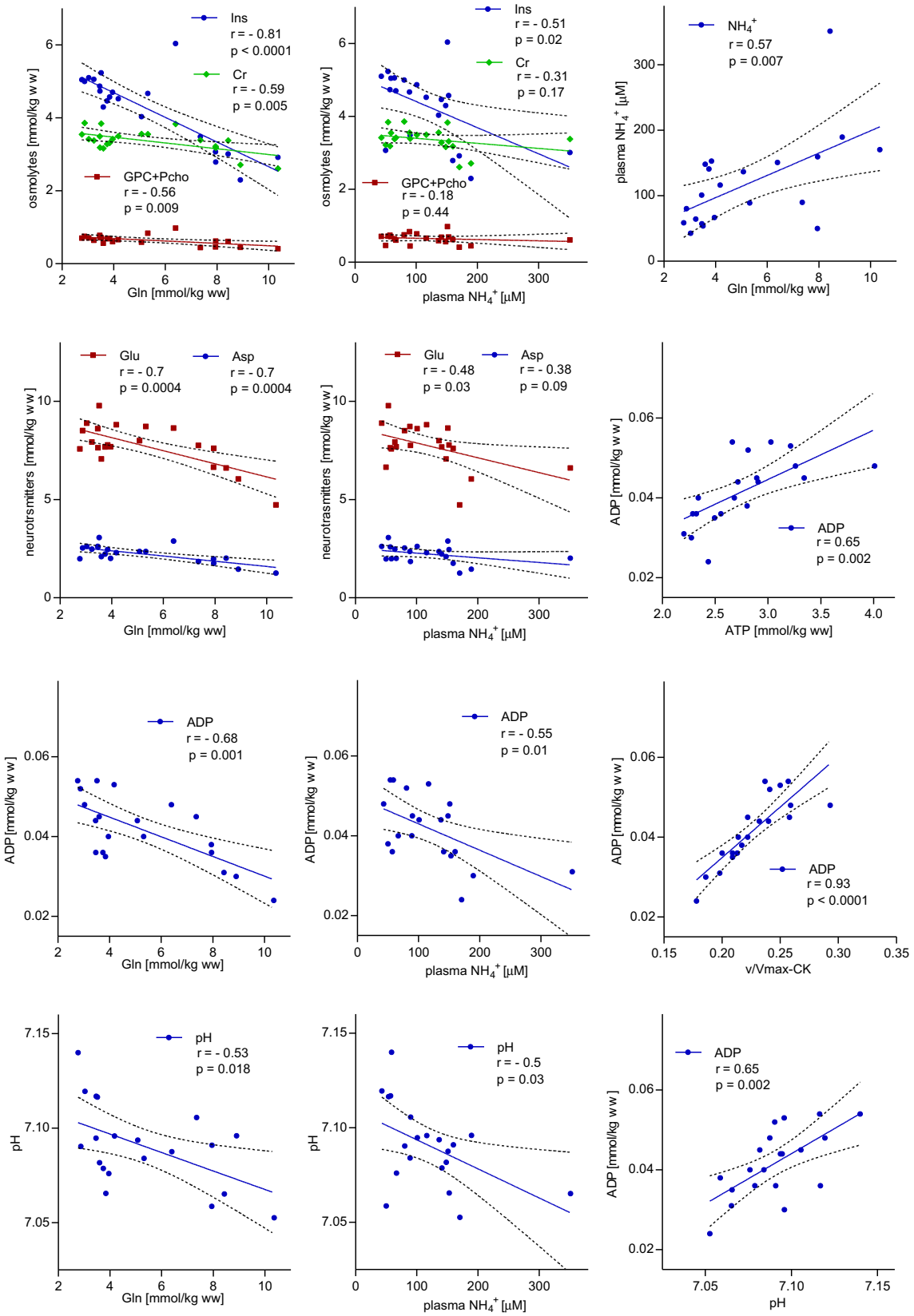
Ins
r = - 0.81
p < 0.0001
Cr
r = - 0.59
p = 0.005
GPC+Pcho
r = - 0.56
p = 0.009
osmolytes [mmol/kg w w]
Gln [mmol/kg ww]
Ins
r = - 0.51
p = 0.02
Cr
r = - 0.31
p = 0.17
GPC+Pcho
r = - 0.18
p = 0.44
plasma NH4+ [µM]
NH4+
r = 0.57
p = 0.007
plasma NH4+ [µM]
Glu
r = - 0.7
p = 0.0004
Asp
r = - 0.7
p = 0.0004
neurotrsmitters [mmol/kg w w]
Glu
r = - 0.48
p = 0.03
Asp
r = - 0.38
p = 0.09
neurotrasmitters [mmol/kg w w]
ADP
r = 0.65
p = 0.002
ADP [mmol/kg w w]
ATP [mmol/kg ww]
ADP
r = - 0.68
p = 0.001
ADP
r = - 0.55
p = 0.01
ADP
r = 0.93
p < 0.0001
v/Vmax-CK
pH
r = - 0.53
p = 0.018
pH
r = - 0.5
p = 0.03
ADP
r = 0.65
p = 0.002
pH

disease, which was also discernible directly from the spectra presented in Fig. 2. Gln increased linearly reaching a 2.5 fold increase at week 8. We measured a gradual decrease of Ins together with other osmolytes as tCho and Cr, in agreement with previously published studies in BDL rats (Chavarria et al. 2013; Bosoi et al. 2014) and CLD patients (Kreis et al. 1992; Bluml et al. 1998; Taylor-Robinson et al. 1999), suggesting a compensatory effect for the osmotic imbalance created by Gln accumulation,. Therefore, as expected, Gln most strongly correlated with Ins, consistent with the fact that Ins is considered as the main astrocytic osmolyte (Lien et al. 1990; Flögel et al. 1995). In the present study, the sum of the main osmolytes (Gln, Ins, tCho, Cr) was not constant over time, showing a 20 % increase at week 8. This progressive yet incomplete osmotic compensation is probably the underlying cause of the observed minimal brain edema associated with chronic HE, as previously shown (Cudalbu et al. 2014; Bosoi et al. 2014). Moreover these changes go along with the appearance of the neurological signs towards the end stage of the disease, as demonstrated by the decrease in locomotor activity in the Open Field task using the same animal model (Leke et al. 2012; Rackayova et al. 2015). Although these findings are not novel, they show that the changes underlying the characteristic high Gln signature of HE occur progressively over the course of time.

The pathogenic mechanisms in HE have been repeatedly associated with disturbances in energy metabolism and neurotransmission systems (in particular glutamatergic and GABA-ergic), however their direct role is still elusive (Lavoie et al. 1987; Häussinger et al. 2000; Braissant 2010; Rama Rao and Norenberg 2012; Schousboe et al. 2014). We used the combined advantages of ultra-short echo time (TE= 2.8 ms) and a high magnetic field to detect additional brain metabolites not previously studied in this model of HE in vivo (i.e. Asp, GABA, Ala, Asc, GSH, PE). In this context, the increase in Gln in our study was further accompanied by a decrease of neurotransmitters Glu and Asp. One explanation for this decrease could be altered neurotransmission. However, a recent in vivo ^{13}C-MRS study performed in our laboratory on the same animal model did not reveal any change in the glutamate-glutamine cycle between astrocytes and neurons (Lanz et al. 2014). Moreover, in contrast to an ex vivo study performed on 6 weeks BDL rats (Leke et al. 2011), no important changes in GABA concentrations were measured in our study. The reduction in Glu could simply be the result of ammonium detoxification driven by increased Gln synthesis from Glu in astrocytes without necessarily affecting neurotransmission. The decline in Glu could in turn induce the decrease in Asp, since the two metabolites are linked by transamination. In addition, it is important to note that Glu and Asp play also a crucial role in malate-aspartate shuttle (Rao and Norenberg 2001).

Increased brain Lac levels are considered as sign of energy disturbances (Rama Rao and Norenberg 2012; Bosoi et al. 2014) with substantial evidence that increased brain Lac is associated with the development of brain edema mainly at comatose stages of HE in ALF models (Chavarria et al. 2010). A recent ex vivo study showed in 6 weeks BDL rats that a rise in Lac (1.7 fold) and not Gln is a primary player in the pathogenesis of brain edema in CLD (Bosoi et al. 2014). Our in vivo longitudinal results are in contrast with these findings since we observed no significant elevation of Lac in rats 8 weeks following BDL, confirming the findings of others in the same animal model and similar brain region (Chavarria et al. 2013). Although our findings are consistent with a previous in vivo study that we performed in the hippocampus (Cudalbu et al. 2014), the different findings of others might be attributed to the fact that different brain regions were investigated, and that the differential vulnerability to CLD of distinct anatomical regions in the brain is incompletely understood. The observed dissimilarities may also be related to technical differences (ex vivo on a liquid nitrogen frozen tissue after decapitation vs in vivo) or to severity of clinical symptoms. Indeed, increased brain Lac seems to be associated with severe HE, while our BDL rats were not in a comatose stage at 8 weeks following BDL. Finally, the kinetics of Gln and ammonium in this previous study (Bosoi et al. 2014) (Gln showed a sharp increase at 2 weeks post BDL and remained seemingly constant thereafter while ammonium increased gradually) a pattern very different to the one measured in our study. Using in vivo MRS, we observed that the rise in Gln can be different among individuals (i.e. gradual increase, initial strong increase followed by a plateau, or late increase only) (Cudalbu et al. 2014) which might eventually lead to differences in brain metabolism.

Cr and PCr are also involved in energy metabolism. One of the main benefits of the high spectral resolution obtained in the present study is the separation of Cr from PCr something never reported in such details in vivo in BDL rats. In our study, PCr showed no change over time while Cr showed a small decrease of −10 % without reaching statistical significance. Without any observable changes in PCr, we tend to believe that the decrease of Cr reflects an osmotic response rather than altered energy metabolism since Cr was recently shown to hold osmotic functions (Bothwell et al. 2002).

^{31}P-MRS is a sensitive method to measure energy metabolites and thus an excellent tool to study cerebral energy metabolism. Previous studies have yielded contradictory results regarding the changes of brain high energy phosphates in CHE. It has been postulated that the discrepancies can be due to the differences in ammonium exposure or severity and timing of clinical symptoms (Rama Rao and Norenberg 2012). In acute hyperammonemia models a decrease in brain ATP has been reported, and has been ascribed to one of two molecular processes: inhibition of phosphorylation or its increased consumption (Kosenko et al. 1994; Ratnakumari et al. 1995; Ott et al. 2005; Rama Rao and Norenberg 2012).

Conversely, in CLD, we observed a non-significant decrease in brain ATP (−10 %), while ADP levels dropped significantly (−28 %) but only at the late stage of the disease. This is in agreement with a decline in measurable ATP and ADP in developing mixed cell aggregates exposed to NH_4Cl (Braissant et al. 2002). Moreover, fluctuations in ATP varied between animals, although this finding did not correlate with brain Gln concentration or plasma ammonium at any time point. Due to its small variation, ATP showed few correlations, the strongest being with ADP, while ADP significantly correlated with the following metabolites: Gln (Fig. 4), Glu, Asp, Ins and Cr. Since there was no change in the $v/V_{max\text{-}ATP}$ the combined decrease in ATP and ADP might suggest defective nucleotide synthesis or increased degradation rather than a decrease in TCA cycle function or mitochondrial respiration. In addition, the total pool of mitochondrial co-enzymes (NAD+NADP) remained constant. Although speculative, one might consider that defective nucleotide synthesis may affect long term brain energy metabolism in a model of CLD.

A few studies using in vivo ^{31}P-MRS in cirrhotic patients have observed decreased ATP concentrations (Bluml et al. 1998; Taylor-Robinson et al. 1999) while others reported higher ADP concentrations (Barbiroli et al. 2002). One of the reasons for these differences can be related to the fact that quantification of the previous ^{31}P-MRS data was performed by fixing either ATP or PCr to equivalent values in all patients. However, as discussed, we observed significant inter-individual variations in ATP concentrations suggesting that a different approach is warranted. By combining in vivo ^{31}P-MRS with ^{1}H-MRS, we were able to use the absolute PCr concentration measured in the same VOI by ^{1}H-MRS as a reference value in the ^{31}P-MRS spectra. Importantly, variations in brain metabolites seem to be region dependent (Lockwood et al. 1986), which may also account for the differences observed from one study to the other.

To further understand the molecular mechanisms underlying the neurological changes associated with type C HE, we analysed the correlations between brain Gln, plasma ammonium and brain energy metabolites. Correlations between plasma ammonium and other measurements remain controversial, especially in CLD where ammonium levels are both lower and more variable than in ALF (Felipo and Butterworth 2002). In our study, the strongest correlation of plasma ammonium was with plasma bilirubin (r=0.65) followed by brain Gln (r=0.57), suggesting that Gln is probably the first metabolite influenced by increased blood ammonium or other circulating compounds not cleared by the diseased liver. Clinically, this finding makes sense since plasma ammonium and bilirubin levels rise with increasing liver disease severity. In light of recent reports, the direct role of bilirubin or bile acids on the brain should be also considered in CLD-induced HE (Quinn et al. 2014). Moreover, plasma ammonium and brain Gln showed similar correlations with other metabolites (i.e. Ins, Glu, ADP), but those with Gln were stronger (see Fig. 4). As previously mentioned, one main advantage of performing MRS at high fields combined with ultra-short echo times is the increased spectral resolution and signal-to-noise ratio allowing the detection of an important number of brain metabolites something never analysed in such details in HE. In this context we observed that compared to ammonium, Gln showed additional and highly significant correlations with tCho, Cr, Asp. Our results indicate that brain Gln, as a result of ammonium detoxification, is still a very important driver of the progressive changes measured in type C HE. However, this is an area in need of further investigation to comprehend how these findings contribute to edema and neurological signs, and to establish the precise molecular mechanisms by which Gln acts in BDL rats. In addition, it should be noted that there are other mechanisms that can lead to brain edema, like oxidative stress, and bile acids.

In conclusion, using in vivo ^{31}P- and ^{1}H-MRS longitudinally in a rat model of type C HE, we have demonstrated mild changes in some energy metabolites. These modifications were observed in end-stage liver disease concomitant with previously shown appearance of brain edema and neurological signs. Therefore, through this unprecedented study using a highly sensitive method in vivo and longitudinally, we can confidently propose that energy metabolism is not one of the major causes of early HE symptoms in the established model of type C HE. In addition, the results of the present study showed that brain Gln remains an important metabolite in type C HE and that osmoregulation impairment caused by Gln accumulation might be a contributing factor to brain edema in BDL rats.

Acknowledgments Supported by Centre d'Imagerie BioMédicale (CIBM) of the UNIL, UNIGE, HUG, CHUV, EPFL, the Leenaards and Jeantet Foundations. EU Grant FP7-PEOPLE-2012-ITN project 316679 TRANSACT. The authors thank Prof. Rolf Gruetter (Centre d'Imagerie BioMédicale (CIBM), École Polytechnique Fédérale de Lausanne (EPFL), Lausanne, Switzerland) for his support and Dr Vladimír Mlynárik (Centre d'Imagerie BioMédicale (CIBM), École Polytechnique Fédérale de Lausanne (EPFL), Lausanne, Switzerland) for his advices on ^{31}P-MRS.

Conflict of Interest The authors declare that they have no conflict of interest.

Appendix

Calculations of energy metabolism parameters

Intracellular pH was calculated based on the difference in resonance frequencies between Pi and PCr signals (δ_{Pi}) in ppm (parts per million) using the Henderson-Hasselbalch equation

$$pH = 6.75 + \log\left[(\delta_{Pi} - 3.29)\Big/(5.68 - \delta_{Pi})\right] \quad (1)$$

(Petroff and Prichard 1985).

Similarly, $[Mg^{2+}]$ was assessed from the difference in resonance frequencies between β-ATP and PCr signals ($\delta_{\beta\text{-ATP}}$) in ppm using equation

$$pMg^{2+} = 4.24 - \log\left[\left(\delta_{\beta-ATP} + 18.58\right)^{0.42} / \left(-15.74 - \delta_{\beta-ATP}\right)^{0.84}\right] \quad (2)$$

(Iotti et al. 1996).

ADP concentration was calculated as

$$[ADP] = ([ATP] \times [Cr]) / ([PCr] \times K_{CK}) \quad (3)$$

with an apparent equilibrium constant of biochemical creatine kinase reaction (K_{CK}) (where the reactant concentrations are the sum of all the ionic and metal complex species at specified pH and $[Mg^{2+}]$) adapted for each particular pH and $[Mg^{2+}]$ of each individual rat as described previously (Golding et al. 1995). [ATP], [Cr] and [PCr] were measured by ^{1}H- and ^{31}P-MRS, pH and $[Mg^{2+}]$ from Eqs. (1) and (2) respectively.

The phosphorylation potential (PP) representing the immediately available high energy phosphate pool was calculated as

$$PP = [ATP] / ([ADP] \times [Pi]) \quad (4)$$

(Veech et al. 1979).

The percentage of the maximal rate of ATP biosynthesis ($v/V_{max\text{-}ATP}$) was calculated according to

$$v/V_{max-ATP} = 1/(1 + 0.2/[ADP] + 0.13/[Pi]) \quad (5)$$

(Veech et al. 1979; Nioka et al. 1987).

Finally the relative rate of CK reaction ($v/V_{max\text{-}CK}$) was determined from

$$v/V_{max-CK} = ([ADP]/([ADP] + K_{m-ADP})) \times ([PCr]/([PCr] + K_{m-PCr})) \quad (6)$$

(Veech et al. 1979), with $K_{m\text{-}ADP}$=0.8 mmol/l and $K_{m\text{-}PCr}$=5.0 mmol/l (Kuby et al. 1954).

References

Barbiroli B, Gaiani S, Lodi R et al (2002) Abnormal brain energy metabolism shown by in vivo phosphorus magnetic resonance spectroscopy in patients with chronic liver disease. Brain Res Bull 59:75–82. doi:10.1016/S0361-9230(02)00839-0

Biecker E, De Gottardi A, Neef M et al (2005) Long-term treatment of bile duct-ligated rats with rapamycin (sirolimus) significantly attenuates liver fibrosis: analysis of the underlying mechanisms. J Pharmacol Exp Ther 313:952–961. doi:10.1124/jpet.104.079616

Blei AT, Córdoba J (2001) Hepatic encephalopathy. Am J Gastroenterol 96:1968–1976. doi:10.1111/j.1572-0241.2001.03964.x

Bluml S, Zuckerman E, Tan J, Ross BD (1998) Proton-decoupled 31P magnetic resonance spectroscopy reveals osmotic and metabolic disturbances in human hepatic encephalopathy. J Neurochem 71: 1564–1576

Bosoi CR, Parent-Robitaille C, Anderson K et al (2011) AST-120 (spherical carbon adsorbent) lowers ammonia levels and attenuates brain edema in bile duct-ligated rats. Hepatology 53:1995–2002. doi:10.1002/hep.24273

Bosoi CR, Zwingmann C, Marin H et al (2014) Increased brain lactate is central to the development of brain edema in rats with chronic liver disease. J Hepatol 60:554–560. doi:10.1016/j.jhep.2013.10.011

Bothwell JH, Styles P, Bhakoo KK (2002) Swelling-activated taurine and creatine effluxes from rat cortical astrocytes are pharmacologically distinct. J Membr Biol 185:157–164. doi:10.1007/s00232-001-0121-2

Braissant O (2010) Ammonia toxicity to the brain: effects on creatine metabolism and transport and protective roles of creatine. Mol Genet Metab 100(Suppl):S53–8. doi:10.1016/j.ymgme.2010.02.011

Braissant O, Henry H, Villard A-M et al (2002) Ammonium-induced impairment of axonal growth is prevented through glial creatine. J Neurosci 22:9810–9820

Braissant O, McLin VA, Cudalbu C (2013) Ammonia toxicity to the brain. J Inherit Metab Dis 36:595–612. doi:10.1007/s10545-012-9546-2

Brusilow SW, Traystman R (1986) Hepatic encephalopathy. N Engl J Med 314:786–787, **author reply 787**

Brusilow SW, Koehler RC, Traystman RJ, Cooper AJL (2010) Astrocyte glutamine synthetase: importance in hyperammonemic syndromes and potential target for therapy. Neurotherapeutics 7:452–470. doi:10.1016/j.nurt.2010.05.015

Butterworth RF (2003) Pathogenesis of hepatic encephalopathy: new insights from neuroimaging and molecular studies. J Hepatol 39: 278–285. doi:10.1016/S0168-8278(03)00267-8

Butterworth RF, Norenberg MD, Felipo V et al (2009) Experimental models of hepatic encephalopathy: ISHEN guidelines. Liver Int 29:783–788. doi:10.1111/j.1478-3231.2009.02034.x

Chavarria L, Oria M, Romero-Gimenez J et al (2010) Diffusion tensor imaging supports the cytotoxic origin of brain edema in a rat model of acute liver failure. Gastroenterology 138:1566–1573. doi:10.1053/j.gastro.2009.10.003

Chavarria L, Oria M, Romero-Giménez J et al (2013) Brain magnetic resonance in experimental acute-on-chronic liver failure. Liver Int 33:294–300. doi:10.1111/liv.12032

Cooper JLA, Plum F (1987) Biochemistry and physiology of brain ammonia. Physiol Rev 67:440–519

Córdoba J, Alonso J, Rovira A et al (2001) The development of low-grade cerebral edema in cirrhosis is supported by the evolution of (1)H-magnetic resonance abnormalities after liver transplantation. J Hepatol 35:598–604

Cudalbu C (2013) In vivo studies of brain metabolism in animal models of Hepatic Encephalopathy using ^{1}H Magnetic Resonance Spectroscopy. Metab Brain Dis 28:167–174. doi:10.1007/s11011-012-9368-9

Cudalbu C, Mlynárik V, Gruetter R (2012) Handling macromolecule signals in the quantification of the neurochemical profile. J Alzheimers Dis 31(Suppl 3):S101–S115. doi:10.3233/JAD-2012-120100

Cudalbu C, Rackayova V, McLin VA, Braissant O (2014) Brain Glutamine, Osmolytes and Edema in a Model of Chronic Hepatic Encephalopathy: in vivo and Londitudinal Measurements using 1H MRS, DTI and Immunofluorescence. 16th ISHEN Meet London. doi: 10.1002/yea.122

Dam G, Keiding S, Munk OL et al (2013) Hepatic encephalopathy is associated with decreased cerebral oxygen metabolism and blood flow, not increased ammonia uptake. Hepatology 57:258–265. doi:10.1002/hep.25995

Davies NA, Wright G, Ytrebø LM et al (2009) L-ornithine and phenylacetate synergistically produce sustained reduction in ammonia and brain water in cirrhotic rats. Hepatology 50:155–164. doi:10.1002/hep.22897

Felipo V, Butterworth RF (2002) Neurobiology of ammonia. Prog Neurobiol 67:259–279

Ferenci P, Lockwood A, Mullen K et al (2002) Hepatic encephalopathy–definition, nomenclature, diagnosis, and quantification: final report of the working party at the 11th World Congresses of Gastroenterology, Vienna, 1998. Hepatology 35:716–721. doi:10.1053/jhep.2002.31250

Flögel U, Niendorf T, Serkowa N et al (1995) Changes in organic solutes, volume, energy state, and metabolism associated with osmotic stress in a glial cell line: a multinuclear NMR study. Neurochem Res 20:793–802

Golding EM, Teague WE, Dobson GP (1995) Adjustment of K' to varying pH and pMg for the creatine kinase, adenylate kinase and ATP hydrolysis equilibria permitting quantitative bioenergetic assessment. J Exp Biol 198:1775–1782

Gruetter R, Tkác I (2000) Field mapping without reference scan using asymmetric echo-planar techniques. Magn Reson Med 43:319–323

Häussinger D (2006) Low grade cerebral edema and the pathogenesis of hepatic encephalopathy in cirrhosis. Hepatology 43:1187–1190. doi:10.1002/hep.21235

Häussinger D, Kircheis G, Fischer R et al (2000) Hepatic encephalopathy in chronic liver disease: a clinical manifestation of astrocyte swelling and low-grade cerebral edema? J Hepatol 32:1035–1038

Hazell AS, Butterworth RF (1999) Hepatic encephalopathy: an update of pathophysiologic mechanisms. Proc Soc Exp Biol Med 222:99–112

Iotti S, Frassineti C, Alderighi L et al (1996) In vivo assessment of free magnesium concentration in human brain by 31P MRS. A new calibration curve based on a mathematical algorithm. NMR Biomed 9:24–32. doi:10.1002/(SICI)1099-1492(199602)9:1<24::AID-NBM392>3.0.CO;2-B

Kale RA, Gupta RK, Saraswat VA et al (2006) Demonstration of interstitial cerebral edema with diffusion tensor MR imaging in type C hepatic encephalopathy. Hepatology 43:698–706. doi:10.1002/hep.21114

Kosenko E, Kaminsky Y, Grau E et al (1994) Brain ATP depletion induced by acute ammonia intoxication in rats is mediated by activation of the NMDA receptor and Na+, K+ ATPase. J Neurochem 63:2172–2178

Kreis R, Farrow N, Ross BD (1991) Localized 1H NMR spectroscopy in patients with chronic hepatic encephalopathy. Analysis of changes in cerebral glutamine, choline and inositols. NMR Biomed 4:109–116

Kreis R, Ross BD, Farrow NA, Ackerman Z (1992) Metabolic disorders of the brain in chronic hepatic encephalopathy detected with H-1 MR spectroscopy. Radiology 182:19–27. doi:10.1148/radiology.182.1.1345760

Kuby SA, Noda L, Lardy HA (1954) Adenosinetriphosphate-creatine transphosphorylase. J Biol Chem 210:65–82

Lai JC, Cooper AJ (1991) Neurotoxicity of ammonia and fatty-acids - differential inhibition of mitochondrial dehydrogenases by ammonia and fatty acyl coenzyme a derivatives. Neurochem Res 16:795–803

Lanz B, Cudalbu C, Mclin V, et al. (2014) Effects of chronic hepatic encephalopathy on brain energy metabolism , studied by in vivo 13 C MRS in rats. 16th ISHEN Meet. London. pp 1–2

Lavoie J, Giguère JF, Layrargues GP, Butterworth RF (1987) Amino acid changes in autopsied brain tissue from cirrhotic patients with hepatic encephalopathy. J Neurochem 49:692–697

Leke R, Bak LK, Iversen P et al (2011) Synthesis of neurotransmitter GABA via the neuronal tricarboxylic acid cycle is elevated in rats with liver cirrhosis consistent with a high GABAergic tone in chronic hepatic encephalopathy. J Neurochem 117:824–832. doi:10.1111/j.1471-4159.2011.07244.x

Leke R, de Oliveira DL, Mussulini BHM et al (2012) Impairment of the organization of locomotor and exploratory behaviors in bile duct-ligated rats. PLoS One 7, e36322. doi:10.1371/journal.pone.0036322

Lien YHH, Shapiro JI, Chan L (1990) Effects of hypernatremia on organic brain osmoles. J Clin Invest 85:1427–1435. doi:10.1172/JCI114587

Lockwood AH, Ginsberg MD, Rhoades HM, Gutierrez MT (1986) Cerebral glucose metabolism after portacaval shunting in the rat. Patterns of metabolism and implications for the pathogenesis of hepatic encephalopathy. J Clin Invest 78:86–95. doi:10.1172/JCI112578

McPhail MJW, Patel NR, Taylor-Robinson SD (2012) Brain Imaging and hepatic encephalopathy. Clin Liver Dis 16:57–72. doi:10.1016/j.cld.2011.12.001

Mlynárik V, Gambarota G, Frenkel H, Gruetter R (2006) Localized short-echo-time proton MR spectroscopy with full signal-intensity acquisition. Magn Reson Med 56:965–970. doi:10.1002/mrm.21043

Mlynárik V, Cacquevel M, Sun-Reimer L et al (2012) Proton and phosphorus magnetic resonance spectroscopy of a mouse model of Alzheimer's disease. J Alzheimers Dis 31(Suppl 3):S87–S99. doi:10.3233/JAD-2012-112072

Nioka S, Chance B, Hilberman M et al (1987) Relationship between intracellular pH and energy metabolism in dog brain as measured by 31P-NMR. J Appl Physiol 62:2094–2102

Ott P, Vilstrup H (2014) Cerebral effects of ammonia in liver disease: current hypotheses. Metab Brain Dis 29:901–911. doi:10.1007/s11011-014-9494-7

Ott P, Clemmesen O, Larsen FS (2005) Cerebral metabolic disturbances in the brain during acute liver failure: From hyperammonemia to energy failure and proteolysis. Neurochem Int 47:13–18. doi:10.1016/j.neuint.2005.04.002

Petroff O, Prichard J (1985) Cerebral intracellular pH by 31P nuclear magnetic resonance. Neurology 35:781–788

Provencher SW (2001) Automatic quantitation of localized in vivo 1H spectra with LCModel. NMR Biomed 14:260–264. doi:10.1002/nbm.698

Quinn M, McMillin M, Galindo C et al (2014) Bile acids permeabilize the blood brain barrier after bile duct ligation in rats via Rac1-dependent mechanisms. Dig Liver Dis 46:527–534. doi:10.1016/j.dld.2014.01.159

Rackayova V, Lanz B, Berset C, et al. (2015) In vivo Longitudinal Measurements of Brain Energy Metabolism in Chronic Hepatic Encephalopathy in a Rat Model using 31P MRS and 1H MRS. 23rd Annu. ISMRM Meet. Toronto. p 1

Rae CD (2014) A guide to the metabolic pathways and function of metabolites observed in human brain 1H magnetic resonance spectra. Neurochem Res 39:1–36. doi:10.1007/s11064-013-1199-5

Rama Rao KV, Norenberg MD (2012) Brain energy metabolism and mitochondrial dysfunction in acute and chronic hepatic encephalopathy. Neurochem Int 60:697–706. doi:10.1016/j.neuint.2011.09.007

Rao KVR, Norenberg MD (2001) Cerebral energy metabolism in hepatic encephalopathy and hyperammonemia. Metab Brain Dis 16:67–78. doi:10.1023/A:1011666612822

Ratnakumari L, Audet R, Qureshi IA, Butterworth RF (1995) Na+, K+ −ATPase activities are increased in brain in both congenital and acquired hyperammonemic syndromes. Neurosci Lett 197:89–92

Schousboe A, Waagepetersen HS, Leke R, Bak LK (2014) Effects of hyperammonemia on brain energy metabolism: controversial findings in vivo and in vitro. Metab Brain Dis. doi:10.1007/s11011-014-9513-8

Shah NJ, Neeb H, Kircheis G et al (2008) Quantitative cerebral water content mapping in hepatic encephalopathy. Neuroimage 41:706–717. doi:10.1016/j.neuroimage.2008.02.057

Taylor-Robinson SD, Sargentoni J, Oatridge A et al (1996) MR imaging and spectroscopy of the basal ganglia in chronic liver disease: correlation of T1-weighted contrast measurements with abnormalities in proton and phosphorus-31 MR spectra. Metab Brain Dis 11:249–268

Taylor-Robinson SD, Buckley C, Changani KK et al (1999) Cerebral proton and phosphorus-31 magnetic resonance spectroscopy in patients with subclinical hepatic encephalopathy. Liver 19:389–398. doi:10.1111/j.1478-3231.1999.tb00067.x

Tkáč I, Starčuk Z, Choi IY, Gruetter R (1999) In vivo 1H NMR spectroscopy of rat brain at 1 ms echo time. Magn Reson Med 41:649–656. doi:10.1002/(SICI)1522-2594(199904)41:4<649::AID-MRM2>3.0.CO;2-G

Tkac I, Henry P-G, Zacharoff L et al (2012) Homeostatic adaptations in brain energy metabolism in mouse models of Huntington disease. J Cereb Blood Flow Metab 32:1977–1988. doi:10.1038/jcbfm.2012.104

Vanhamme L, van den Boogaart A, Van Huffel S (1997) Improved method for accurate and efficient quantification of MRS data with use of prior knowledge. J Magn Reson 129:35–43

Veech RL, Lawson JW, Cornell NW, Krebs HA (1979) Cytosolic phosphorylation potential. J Biol Chem 254:6538–6547

Zwingmann C (2007) The anaplerotic flux and ammonia detoxification in hepatic encephalopathy. Metab Brain Dis 22:235–249. doi:10.1007/s11011-007-9069-y

Zwingmann C, Butterworth R (2005) An update on the role of brain glutamine synthesis and its relation to cell-specific energy metabolism in the hyperammonemic brain: further studies using NMR spectroscopy. Neurochem Int 47:19–30. doi:10.1016/j.neuint.2005.04.003